Inelastic Scattering by Deformed Nuclei*

J. S. BLAIR, D. SHARP,† AND L. WILETS
University of Washington, Seattle, Washington
(Received September 13, 1961)

The techniques of the sharp and rounded cutoff models for elastic scattering have been extended to the calculation of nuclear monopole and quadrupole excitation in the adiabatic approximation. In the case of scattering from nuclei with quadrupole deformations, a spheroidal coordinate system is introduced where one of the coordinate ellipsoids coincides with the nuclear surface; the wave equation separates outside the range of the nuclear potential. Formal expressions and results of numerical calculations for the cross sections are presented for a case where simple assumptions are made about the functional form of the partial wave amplitudes and where only terms linear in nuclear deformation are retained. One limit of the form for the spherical partial wave amplitudes leads to a sharp-cutoff model which goes over into the Fraunhofer results for moderate and large values of the critical angular momentum. It is found that graphs of the excitation cross section (and to a lesser extent the elastic scattering cross section) fall into a single-parameter family of "universal curves" when plotted against (scattering angles)$\times$(critical angular momentum$+\frac{1}{2}$). The single parameter is (thickness of transition region in l space) $\div$ (critical angular momentum). No detailed comparisons with experiment are made, but the model is capable of reproducing the qualitative results of alpha-particle scattering at energies well above the Coulomb barrier.

I. INTRODUCTION

THE adiabatic approximation[1–4] is frequently a useful and appropriate theoretical tool with which to investigate inelastic scattering from nuclei. The observed inter-relations between elastic and inelastic cross sections are more easily understood through use of this approximation[4–7] than appears evident with other procedures. It is noteworthy that the adiabatic approximation is particularly applicable to collective nuclear surface excitations, since it appears that the low-lying levels most strongly excited through inelastic scattering are of this type.[8] Comparison between theoretical calculations performed with and without the use of the adiabatic approximation have indicated that the range of validity of the adiabatic approximation is wider than a superficial study would lead one to expect.[9,10]

When the adiabatic approximation is valid, the amplitude for a particle to scatter from initial state a to final state b may be written as

$$T_{ba}(\text{adiab})=\langle\Phi_b(\alpha)\,|\,t(\mathbf{k}_b,\mathbf{k}_a,\alpha)\,|\,\Phi_a(\alpha)\rangle, \qquad (1)$$

where $t(\mathbf{k}_b,\mathbf{k}_a,\alpha)$ is the exact scattering amplitude for the elastic scattering problem ($k_a=k_b$) with static α. Thus, both the problem of true elastic and inelastic scattering reduce to a study of the elastic scattering amplitude for fixed collective coordinates.

The most successful model for the description of elastic scattering of nuclear projectiles from spherical nuclei has been the optical model. For complex nuclear projectiles such as alpha particles, however, the nucleus appears, to a good approximation, as a sharply defined absorbing sphere and thus a variety of extremely simple models have also enjoyed fair success in matching the elastic cross sections (particularly at low orders in the diffraction pattern). Perhaps the most elementary of these models is one familiar from the study of physical optics, namely, Fraunhofer diffraction due to a black circular disk.[11,12]

A nearly equivalent model is the sharp-cutoff model[13] in which it is assumed that the amplitudes of the outgoing partial waves η_l undergo, at a critical angular momentum L, a sharp transition from zero to their value in the absence of an absorbing nucleus; for large L, zero charge, and small scattering angles, the resulting scattering amplitude is equivalent to the Fraunhofer black-disk result. Generalizations of the sharp-cutoff model, in which there is a smoothed transition in the value of η_l, have been able to fit quantitatively even large-angle elastic-scattering cross sections.[14]

It is not difficult to apply the Fraunhofer diffraction treatment to an absorbing nucleus whose surface is deformed from spherical shape. The resulting scattering amplitude will be a function of the (dynamical) collective nuclear surface coordinates and thus, according to Eq. (1), will lead to inelastic scattering. Drozdov[2] and Inopin[3] introduced this procedure for the case of ellipsoidally deformed nuclei and one of the present authors[4] generalized the method to deformations of arbitrary multipolarity. Exceedingly simple expressions for scattering cross sections are obtained when two further approximations are made in addition to the

* Supported in part by the U. S. Atomic Energy Commission.
† 1959 summer visitor, now at the California Institute of Technology, Pasadena, California.
[1] D. M. Chase, Phys. Rev. **104**, 838 (1956).
[2] S. I. Drozdov, J. Exptl. Theoret. Phys. (U.S.S.R.) **28**, 734 (1955); **28**, 736 (1955) [translation; Soviet Phys. JETP **1**, 588, 591 (1955)].
[3] E. V. Inopin, J. Exptl. Theoret. Phys. (U.S.S.R.) **31**, 901 (1956) [translation; Soviet Phys. JETP **4**, 784 (1957)].
[4] J. S. Blair, Phys. Rev. **115**, 928 (1959).
[5] D. K. McDaniels, J. S. Blair, S. W. Chen, and G. W. Farwell, Nuclear Phys. **17**, 614 (1960).
[6] J. S. Blair, G. W. Farwell, and D. K. McDaniels, Nuclear Phys. **17**, 641 (1960).
[7] J. S. Blair and L. Wilets, Phys. Rev. **121**, 1493 (1961).
[8] B. L. Cohen, Phys. Rev. **105**, 1549 (1957).
[9] D. M. Chase, L. Wilets, and A. R. Edmonds, Phys. Rev. **110** 1080 (1958).
[10] E. Rost and N. Austern, Phys. Rev. **120**, 1375 (1960).
[11] See, for example, P. M. Morse and H. Feshbach, *Methods of Theoretical Physics* (McGraw-Hill Book Company, Inc., New York, 1953), p. 1552.
[12] A. I. Yavin and G. W. Farwell, Nuclear Phys. **12**, 1 (1959).
[13] J. S. Blair, Phys. Rev. **95**, 1218 (1954).
[14] J. A. McIntyre, K. H. Wang, and L. C. Becker, Phys. Rev. **117**, 1337 (1960).

adiabatic and Fraunhofer diffraction approximations: (1) The nucleus is considered to be black within a strong absorption surface $R(\theta',\phi')$ which is related to the collective surface coordinates $\alpha_{\lambda\mu}$ through the familiar expression $R(\theta',\phi')=R_0[1+\sum \alpha_{\lambda\mu}Y_{\lambda\mu}(\theta',\phi')]$. (2) The scattering amplitude is expanded only to terms linear in $\alpha_{\lambda\mu}$.

The purpose of the present paper is to present an extension of the cutoff models, sharp or smoothed, to inelastic scattering. Crucial use is again made of the adiabatic approximation. The advantages of these models over that described in the paragraph above are: (a) the Fraunhofer diffraction approximation, which is trustworthy only at small scattering angles, is circumvented. (b) The sharp-edged strong-absorption radius may now be softened in the sense that it is possible to spread a transition from complete to no absorption over several partial waves.

Although the model is easily formulated for an arbitrary magnitude of deformation, the mathematics is simple only in the approximation that terms linear in the deformation parameter are retained in the scattering amplitude [which is assumption (2) of the previous paragraph]. The cutoff model is feasible for monopole and quadrupole excitations only because the free wave equation is separable in spherical and spheroidal coordinates. The model does not appear to generalize to higher order deformations.

We appreciate that the model has its limitations. The linear deformation approximation is suspect, particularly at the large angles. An indication of the importance of terms high order in the deformation may be obtained through expansion of the Fraunhofer scattering amplitude for a sharp edged ellipsoid of arbitrary deformation[2]; it is found[4] that the most relevant expansion parameter is the quantity $(\beta kR_0\theta)$, where β is a measure of the permanent deformation; thus the expansion converges poorly at large orders of the diffraction pattern. Effects due to nonlinear terms in the scattering amplitude have been observed experimentally[15]; the angular distributions of alpha particles which excite some $0^+ \rightarrow 4^+$ transitions are in qualitative agreement with theories in which terms of second order in the collective coordinates occurring in the scattering amplitudes are responsible for the transition.[16,17]

A further defect of our method is the prescription for obtaining partial wave amplitudes which, although physically plausible, contains phenomenological parameters; a more fundamental procedure would be, for example, to obtain these partial wave amplitudes from the solution of Schrödinger's equation with a complex potential.

A generalization of the optical model to treat inelastic (neutron) scattering from deformed nuclei has been carried out.[9] In that model, the Schrödinger equation was integrated as a set of coupled differential equations corresponding to the various reaction channels. The model is characterized by the parameters of the complex potential, surface thickness and shape, and the moment of inertia; the adiabatic approximation is not made. Indeed, the inelastic cutoff and Fraunhofer models may be regarded as approximations or simulations to the inelastic optical model. The advantages of the simpler models are that they are characterized by fewer parameters and require considerably less effort for numerical computation.

In Sec. II, monopole excitation is considered as a first example of inelastic scattering in the cutoff model. Section III gives a formulation of the scattering problem in spheroidal coordinates, while in Sec. IV the scattering formulas for quadrupole excitation are developed. Numerical results are presented in Sec. V. Possible extensions of the model are discussed in Sec. VI.

II. MONOPOLE EXCITATION

In this section the techniques to be used in the paper will be exhibited for the simple case of monopole excitation, in which geometrical complications arising from quadrupole deformations are absent.

The general expression for the elastic scattering amplitude of a spinless projectile incident on a spherical target is

$$f(\theta)=-(2ik)^{-1}\sum_{l=0}^{\infty}(2l+1)(1-\eta_l)P_l(\cos\theta), \qquad (2)$$

where $k(\equiv 1/\lambda\!\!\!^{-})$ is the relative wave number, θ is the scattering angle in the center-of-mass system, $P_l(\cos\theta)$ is the Legendre polynomial of order l, and η_l is the amplitude of the lth outgoing partial wave.

The sharp cutoff approximation (in the case where the Coulomb interaction is neglected) consists in the assumption that

$$\begin{aligned}\eta_l&=0 \quad \text{for} \quad l<L,\\ \eta_l&=1 \quad \text{for} \quad l>L,\end{aligned} \qquad (3)$$

where the critical angular momentum L, which need not be an integer, is related to the sharp cutoff radius by[18]

$$(kR)^2\equiv L(L+1). \qquad (4)$$

If $l=L$ it will be assumed that $\eta_L=\frac{1}{2}$.

[15] R. Beurtey, P. Catillon, R. Chaminade, M. Crut, H. Faraggi, A. Papineau, J. Saudinos, and J. Thirion, Compt. rend. **252**, 1756 (1961).

[16] S. I. Drozdov, J. Exptl. Theoret. Phys. (U.S.S.R.) **38**, 499 (1960) [translation; Soviet Phys. JETP **11**, 362 (1960)].

[17] R. H. Lemmer, A. de Shalit, and N. S. Wall (to be published).

[18] The correspondence between the "nuclear radius" R, and the critical angular momentum, L, given in Eq. (4) is, as indicated, a matter of definition. The nuclear radius has been defined as that radius at which the Lth partial wave has its classical turning point in the absence of any nuclear potential. A similar statement applies for the quadrupole deformation problem concerning the correspondence between the "nuclear surface" ξ_c, and the critical angular momentum L, given by Eq. (46). The question naturally arises: What is the connection between the cutoff parameters L and R and those which characterize the optical potential for the

Smoothed cutoff models,[14,19] in which there is a more gradual transition from complete to no absorption, not only seem more realistic but have also provided a better fit to observed elastic α-particle cross sections. Further justification for smoothed cutoff models is provided by the form of $|\eta_l|$ resulting from optical model calculations[20,21] and by arguments relating to barrier penetrabilities.

As a statement of the smoothed cutoff approximation, it is assumed that η_l is a smooth, monotonic function of the difference $(l-L)$. The critical angular momentum L is again related to a critical radius R by Eq. (4). The form of $\eta_l=\eta(l-L)$ is restricted by requiring that $\eta(0)=\frac{1}{2}$.

Now consider a monopole deformation, i.e., a deformation which simply increases the nuclear radius by an amount δ. It is assumed that the critical (strong absorption) radius entering the scattering problem is correspondingly increased $(R=R_0+\delta)$, so that

$$L\cong L_0+k\delta. \tag{5}$$

Here R_0 and L_0 are, respectively, the critical radius and angular momentum for zero deformation. If the amplitude of lth outgoing wave, $\eta(l-L)$ is now expanded to first order in the deformation δ, one finds

$$\eta(l-L)\cong\eta(l-L_0)-k\delta\eta'(l-L_0), \tag{6}$$

so that

$$f(\theta)\cong-(2ik)^{-1}\Big\{\sum_l(2l+1)[1-\eta(l-L_0)]P_l(\cos\theta) +\delta\sum_l(2l+1)\frac{d\eta(l-L_0)}{dl}P_l(\cos\theta)\Big\}. \tag{7}$$

The monopole deformation δ will now be regarded as a collective coordinate corresponding to the "breathing mode" of nuclear motion. The inelastic scattering cross section for excitation of this mode is then given, according to the adiabatic approximation [Eq. (1)], as

$$\frac{d\sigma}{d\Omega}(0\to 0)=|\langle b|\delta|a\rangle\sum_l(l+\tfrac{1}{2})\eta'(l-L_0)P_l(\cos\theta)|^2. \tag{8}$$

A particularly simple result emerges when the transition region is sufficiently broad so that the sum over l may be replaced by an integral and yet narrow enough so that the product $(l+\frac{1}{2})P_l(\cos\theta)$ may be taken outside the integral and replaced by its value at the point where $d\eta_l/dl$ is a maximum. A form of $\eta(l-L_0)$ is assumed for which $\eta(l-L_0)$ is symmetric about L_0, and such that the derivative is a maximum at L_0. Then the cross section, Eq. (8), becomes

$$\frac{d\sigma}{d\Omega}(0\to 0)\cong|\langle b|\delta|a\rangle|^2(L_0+\tfrac{1}{2})^2|P_{L_0}(\cos\theta)|^2, \tag{9}$$

since $\int\eta'(l-L_0)dl=1$.

At small angles the Legendre polynomials are well approximated by zeroth order Bessel functions: $P_l(\cos\theta)\to J_0[(l+\frac{1}{2})\theta]$. Thus, in the forward direction, the above derivation yields the Fraunhofer result[4]

$$\frac{d\sigma}{d\Omega}(0\to 0)\cong(kR_0)^2|\langle b|\delta|a\rangle|^2J_0^2(kR_0\theta). \tag{10}$$

At this point it is of interest to mention the corresponding results for elastic cross sections. For a sharp transition centered at L, where L is an integer, one finds

$$\sum_{l=0}^{\infty}(2l+1)[1-\eta(l-L)]P_l(\cos\theta) \cong\sum_{l=0}^{L-1}(2l+1)P_l(\cos\theta)+\tfrac{1}{2}(2L+1)P_L(\cos\theta). \tag{11}$$

When use is made of the recursion relation $(2l+1)P_l=P_{l+1}'-P_{l-1}'$, the elastic cross section becomes

$$d\sigma_{el}/d\Omega=(1/4k^2)[P_L'+\tfrac{1}{2}(P_{L-1}'+P_{L+1}')]^2, \tag{12}$$

the primes denoting differentiation with respect to $\cos\theta$. In the forward direction, the Legendre polynomials are again approximated by Bessel functions to obtain

$$d\sigma_{el}/d\Omega\cong(kR_0^2)^2|J_1(kR_0\theta)/(kR_0\theta)|^2, \tag{13}$$

so that the elastic cross section reduces to the familiar Fraunhofer black-disk formula.

Finally, in the extreme forward direction $(\theta=0)$, the elastic cross section becomes simply

$$d\sigma_{el}/d\Omega\cong(1/4k^2)[(L+\tfrac{1}{2})^2+\tfrac{1}{4}]^2\cong(kR_0^2)^2/4. \tag{14}$$

---

nucleus? It is our belief that the maximum value of the real part of the total potential, nuclear plus centrifugal, for the critical angular momentum L in the surface region is very closely equal to the available energy E. This correspondence was demonstrated in reference (26) for elastic alpha-particle scattering through comparison of observed sharp-cutoff angular momenta and those determined by application of the above criterion to the "best fit" optical potentials. The statement also appears plausible from consideration of nuclear barrier penetrabilities. Indeed, it has been pointed out that for a barrier which may be approximated as an inverted parabola, the barrier penetration probability is exactly $\frac{1}{2}$ when the top of the barrier equals E [D. L. Hill and J. A. Wheeler, Phys. Rev. **89**, 1102 (1953)]. Application of the above criterion to a square well optical potential leads to the result that the radius of the well equals the R of Eq. (4). When this criterion is applied, however, to a diffuse potential which decreases exponentially with fall off distance d, it is found that R is energy dependent [see reference (26)]; the magnitude of the nuclear potential at the cutoff radius R is relatively small, being of the order $(d/R)E$. For a diffuse potential of the Saxon form it is easy to see that the values of the cutoff radii are usually much larger than typical values for the midpoint radii of the potential. An additional point to be noted is that for some purposes—e.g., to obtain a WKB solution of the wave equation—it is better to make the substitution $l(l+1)\to(l+\frac{1}{2})^2$. Whether, $L(L+1)$ or $(L+\frac{1}{2})^2$ is used in Eqs. (4) and (46) does not affect the subsequent results except insofar as it does alter the interpretation of the nuclear radius obtained from analysis of experimental results; in practice, the difference is negligible.

[19] K. R. Greider and A. E. Glassgold, Ann. Phys. **10**, 100 (1960).

[20] W. B. Cheston and A. E. Glassgold, Phys. Rev. **106**, 1215 (1957).

[21] N. Austern (to be published).

The Fraunhofer results lie close to the elastic and inelastic cross sections given by Eqs. (9) and (12) for rather large values of the scattering angle. The general features are similar to those discussed for quadrupole deformation in Sec. V.

Computations of the monopole cross section using a smooth form for η_l in Eq. (8) have not been carried out in this paper.

III. FORMULATION OF THE SCATTERING PROBLEM IN SPHEROIDAL COORDINATES

Inelastic scattering from a nucleus with quadrupole surface deformation may be treated in a manner similar to that employed for monopole excitations. The mathematical apparatus required, however, is now more complicated since it is necessary that the problem be formulated in spheroidal coordinates. There is an extensive literature concerning solutions of the wave equation in these coordinates[22,23] and general expressions for the scattering cross sections in the adiabatic approximation have been given by Inopin.[24] We find it desirable to recapitulate some of this material in the present section. In this development attention is called to some special relations, valid to first order in the deformation parameter, which at a later stage make ours a manageable calculation.

A. Separation of the Wave Equation

Prolate spheroidal coordinates are defined in terms of rectangular coordinates by the relations

$$\xi=(r_1+r_2)/a, \tag{15a}$$

$$\eta=(r_1-r_2)/a, \tag{15b}$$

$$\phi=\tan^{-1}(y/x), \tag{15c}$$

where $r_{1,2}=[(z\pm\frac{1}{2}a)^2+x^2+y^2]^{\frac{1}{2}}$. The variables are limited to the ranges:

$$\begin{aligned} 1\leq\xi<\infty,\\ -1\leq\eta\leq 1,\\ 0\leq\phi<2\pi. \end{aligned} \tag{16}$$

Surfaces of constant ξ are prolate spheroids with foci at $z=\pm\frac{1}{2}a$; surfaces of constant η are hyperboloids of revolution with foci at $\pm\frac{1}{2}a$. In the limit $r_{1,2}\rightarrow\infty$ or $a\rightarrow 0$, these coordinates are related to the spherical coordinates r and θ as follows:

$$\begin{aligned} \xi&\rightarrow 2r/a,\\ \eta&\rightarrow\cos\theta. \end{aligned} \tag{17}$$

In the absence of potential, the wave equation,

$$(\nabla^2+k^2)\psi=0, \tag{18}$$

is separable in spheroidal coordinates. If one assumes for ψ the form $\psi=J(\xi)\,\mathrm{Ps}(\eta)\Phi(\phi)$, Eq. (18) yields for J, Ps, and Φ the equations:

$$\left\{\frac{d}{d\xi}\left[(\xi^2-1)\frac{d}{d\xi}\right]-\Lambda+h^2\xi^2-\frac{m^2}{\xi^2-1}\right\}J(\xi)=0, \tag{19a}$$

$$\left\{\frac{d}{d\eta}\left[(1-\eta^2)\frac{d}{d\eta}\right]+\Lambda-h^2\eta^2-\frac{m^2}{1-\eta^2}\right\}\mathrm{Ps}(\eta)=0, \tag{19b}$$

$$\{d^2/d\phi^2+m^2\}\Phi(\phi)=0. \tag{19c}$$

Λ and m are separation constants, and $h\equiv\frac{1}{2}ak$. The separation constants Λ are nonintegral but form a discrete set, each element of which may be labeled by an integer l as well as by m; the manner in which this correspondence is made will be apparent from Eqs. (20) and (21) to follow.

Normalized spheroidal harmonics $\mathcal{Y}_{lm}$ are defined by

$$\begin{aligned} \mathrm{Ps}_{lm}(h;\eta)\Phi_m(\phi)\propto\mathcal{Y}_{lm}(h;\vartheta,\phi)\\ =\textstyle\sum_{l'}A_{ll'}{}^{m}Y_{l'm}(\vartheta,\phi), \end{aligned} \tag{20}$$

where $\vartheta\equiv\cos^{-1}\eta$, $\Phi_m=(2\pi)^{-\frac{1}{2}}e^{im\phi}$, and $Y_{l'm}$ are spherical harmonics. Moreover, l and l' are of the same parity.

Formal expansion of the coefficients $A_{ll'}{}^{m}(h)$ and the separation constants $\Lambda=\Lambda_{lm}(h)$ in powers of h^2 gives

$$A_{ll'}{}^{m}(h)=\delta_{ll'}+h^2\alpha_{ll'}{}^{m}+O(h^4), \tag{21a}$$

$$\Lambda_{lm}(h)=l(l+1)+h^2\lambda_{lm}+O(h^4). \tag{21b}$$

The coefficients $\alpha_{ll'}{}^{m}$ and λ_{lm} may be determined by the application of standard perturbation theory to Eq. (19b), with $h^2\eta^2=h^2\cos^2\vartheta$ as the perturbing term. This yields, to lowest order,

$$\begin{aligned} \alpha_{ll'}{}^{m}=-\alpha_{l'l}{}^{m}&=\int Y_{l'm}{}^{*}\cos^2\vartheta\,Y_{lm}d\Omega/[l(l+1)-l'(l'+1)]\\ &=\frac{2}{3}\left(\frac{2l+1}{2l'+1}\right)^{\frac{1}{2}}\frac{(l\,2\,m\,0|l'\,m)(l\,2\,0\,0|l'\,0)}{l(l+1)-l'(l'+1)}, \end{aligned}$$

$$(l'=l\pm 2), \tag{22a}$$

and

$$\begin{aligned} \lambda_{lm}&=\int Y_{lm}{}^{*}\cos^2\vartheta\,Y_{lm}d\Omega\\ &=\tfrac{2}{3}(l\,2\,m\,0|l\,m)(l\,2\,0\,0|l\,0)+\tfrac{1}{3}. \end{aligned} \tag{22b}$$

The regular and irregular solutions of the "radial" equation (19a) are the spheroidal functions $\mathrm{je}_{lm}(h,\xi)$ and $\mathrm{ne}_{lm}(h,\xi)$ which approach the spherical radial functions not only as $h\rightarrow 0$, but also (nontrivially) as $\xi\rightarrow\infty$ with h fixed:

$$\begin{aligned} \mathrm{je}_{lm}(h,\xi)&\underset{\xi\rightarrow\infty}{\longrightarrow}j_l(h\xi)\rightarrow(h\xi)^{-1}\sin[h\xi-\tfrac{1}{2}\pi l],\\ \mathrm{ne}_{lm}(h,\xi)&\underset{\xi\rightarrow\infty}{\longrightarrow}n_l(h\xi)\rightarrow(h\xi)^{-1}\sin[h\xi-\tfrac{1}{2}\pi(l+1)]. \end{aligned} \tag{23}$$

[22] P. M. Morse and H. Feshbach, *Methods of Theoretical Physics* (McGraw-Hill Book Company, Inc., New York, 1953), p. 1502.
[23] *Higher Transcendental Functions* edited by A. Erdelyi (McGraw-Hill Book Company, Inc., New York, 1955), Vol. III.
[24] E. V. Inopin, J. Exptl. Theoret. Phys. (U.S.S.R.) **34**, 1455 (1958) [translation; Soviet Phys. JETP **7**, 1007 (1958)].

This permits a phase-shift representation of the scattering problem in the spheroidal representation. Furthermore, since the spheroidal coordinates $\vartheta=\cos^{-1}\eta$ and ξ approach the spherical coordinates θ and $2r/a$ at large radii, the spheroidal phase shifts can readily be incorporated into the spherical formulation of the scattering problem.

B. Expansion of a Plane Wave

Let us recall the expansion in spherical harmonics of a plane wave incident along the space-fixed z direction in terms of a coordinate system rotated with respect to the space-fixed system. This is:

$$e^{ikz}=\sum_l i^l(2l+1)j_l(kr)P_l(\cos\theta)$$
$$=4\pi\sum_{lm} i^l j_l(kr)Y_{lm}{}^*(-\beta,-\gamma)Y_{lm}(\theta',\phi'), \quad (24)$$

where θ is the angle between the space-fixed z axis and the field point; α, β, $\gamma(\equiv\mathbf{N})$ are the Eulerian angles which rotate the space-fixed coordinate system into the body-fixed system and θ', ϕ' give the orientation of the field point with respect to the body-fixed axes.

In complete analogy, the expansion of a plane wave in spheroidal harmonics is given by:

$$e^{ikz}=4\pi\sum_{lm} i^l \mathrm{je}_{lm}(h,\xi')$$
$$\times\mathcal{Y}_{lm}{}^*(h;-\beta,-\gamma)\mathcal{Y}_{lm}(h;\vartheta',\phi'), \quad (25)$$
$$\underset{r\to\infty}{\longrightarrow} 2\pi(kr)^{-1}\sum_{lm} i^{l+1}[e^{-i(kr-\frac{1}{2}\pi l)}-e^{+i(kr-\frac{1}{2}\pi l)}]$$
$$\times\mathcal{Y}_{lm}{}^*(h;-\beta,-\gamma)\mathcal{Y}_{lm}(h;\theta',\phi'). \quad (26)$$

In these formulas, the notation of the previous section has been altered by placing primes on the spheroidal coordinates when they refer to body-fixed axes.

C. The Scattering Amplitude

In terms of spheroidal Hankel functions, $\mathrm{he}_{lm}{}^{(\pm)}=\mathrm{je}_{lm}\pm i\,\mathrm{ne}_{lm}$, the general solution of the wave equation which is asymptotically a plane wave, has the form (outside the region of the potential)

$$\Psi=2\pi\sum_{lm} i^l[\mathrm{he}_{lm}{}^{(-)}+\eta_{lm}\,\mathrm{he}_{lm}{}^{(+)}]\mathcal{Y}_{lm}{}^*(h;-\beta,-\gamma)\mathcal{Y}_{lm}(h;\vartheta',\phi')\underset{r\to\infty}{\longrightarrow}$$
$$(2\pi)(kr)^{-1}\sum_{lm} i^{l+1}[e^{-i(kr-\frac{1}{2}\pi l)}-\eta_{lm}e^{i(kr-\frac{1}{2}\pi l)}]\mathcal{Y}_{lm}{}^*(h;-\beta,-\gamma)\mathcal{Y}_{lm}(h;\theta',\phi). \quad (27)$$

The adiabatic scattering amplitude is given by[24]

$$f(\theta,\phi;\mathbf{N})=\lim_{r\to\infty} re^{-ikr}[\Psi-e^{ikz}] \quad (28)$$
$$=2\pi i\lambda\sum_{lm}(1-\eta_{lm})\mathcal{Y}_{lm}{}^*(h;-\beta,-\gamma)\mathcal{Y}_{lm}(h;\theta,\phi')$$
$$=2\pi i\lambda\sum_{lm}(1-\eta_{lm})\sum_{l'l''}A_{ll'}{}^m A_{ll''}{}^m Y_{l'm}{}^*(-\beta,-\gamma)Y_{l''m}(\theta',\phi'). \quad (29)$$

It should be borne in mind that dependence on nuclear orientation is contained implicitly in θ', ϕ' as well as in the Eulerian angles (β,γ).

According to Eq. (1) the amplitude for scattering from the nuclear state (I_0M_0) to the state (IM) is given, in the adiabatic approximation, by

$$f_{IM;I_0M_0}(\theta,\phi)=\langle IM|f(\theta,\phi;\mathbf{N})|I_0M_0\rangle, \quad (30)$$

where, in the notation of Rose[25]

$$|IM\rangle=\left(\frac{2I+1}{8\pi^2}\right)^{\frac{1}{2}}D_{M0}{}^{I*}(\alpha,\beta,\gamma). \quad (31)$$

for a $K=0$ rotational state. A typical term in Eq. (30) for a $(0,0)\to(I,M)$ transition requires evaluation of the integral

$$\langle IM|Y_{l'm}{}^*(-\beta,-\gamma)Y_{l''m}(\theta',\phi')|0\,0\rangle=\left\langle IM\left|\left(\frac{2l'+1}{4\pi}\right)^{\frac{1}{2}}D_{0m}{}^{l'*}(\alpha,\beta,\gamma)\sum_{m'}D_{m'm}{}^{l''}(\alpha,\beta,\gamma)Y_{l''m'}(\theta,\phi)\right|0\,0\right\rangle$$
$$=\left[\frac{1}{4\pi}\frac{2I+1}{2l'+1}\right]^{\frac{1}{2}}(l''\,I\,-M\,M|l'\,0)(l''\,I\,m\,0|l'\,m)Y_{l'',-M}(\theta,\phi). \quad (32)$$

To obtain Eq. (32) use has been made of the relation[25]

$$\int D_{k_1m_1}{}^{j_1}D_{k_2m_2}{}^{j_2}D_{k_3m_3}{}^{j_3*}d\mathbf{N}=[(8\pi^2)/(2j_3+1)](j_1j_2k_1k_2|\,j_3k_3)(j_1j_2m_1m_2|\,j_3m_3). \quad (33)$$

[5] M. E. Rose, *Elementary Theory of Angular Momentum* (John Wiley & Sons, Inc., New York, 1957), p. 60.

Thus one obtains for the scattering amplitude:

$$f_{IM;00}(\theta,\phi) = (\pi)^{\frac{1}{2}} i\lambda \sum_{ll'l''} (1-\eta_{lm}) A_{ll'}{}^{m} A_{ll''}{}^{m} [(2I+1)/(2l'+1)]^{\frac{1}{2}} \times (l''\, I\, -M\, M\,|\, l'\, 0)(l''\, I\, m\, 0\,|\, l'\, m) Y_{l'',-M}(\theta,\phi). \quad (34)$$

Note added in proof. The explicit form of the scattered wave given in Eq. (28) *et seq.* assumes the existence of a nuclear potential, separable in spheroidal coordinates, of the form $f[\frac{1}{2}(r_1+r_2)]/r_1r_2 = 4f(\frac{1}{2}a\xi)/[a^2(\xi^2-\eta^2)]$. Although this form possesses unphysical singularities at the two foci, we shall apply our procedures only to nuclear models for which there is strong absorption in the nuclear interior, in which case such singularities should be of little consequence for the scattering amplitude. The equipotential surfaces for this form of the potential do not coincide with surfaces of constant ξ; however, for f a smooth function, the equipotential surfaces, through first order in the deformation, are still spheroids, characterized by ϵ(potential) $= \epsilon$(coord, system)$[1-(2f/f'R)/(1-2f/f'R)]$, [cf. Eq. (56) for the definition of ϵ]. Thus for

$$f \propto \exp[-\tfrac{1}{2}(r_1+r_2)/c]$$

in the surface region, the ϵ is "renormalized" by the factor $(1+2c/R)$. The ϵ and β_2 of Eq. (57) are characteristic of the coordinate system, not of the nuclear potential.

Equation (34) is a specialization of Eq. (42) in Inopin's paper[24] to the case of a separable nuclear potential. We wish to thank Professor Inopin for pointing out an erroneous statement in our original manuscript concerning these equations.

IV. EVALUATION OF THE SCATTERING AMPLITUDE FOR QUADRUPOLE EXCITATION

At this point the linear approximation is made in the evaluation of the scattering amplitude Eq. (34); that is, terms higher than first power in the parameter h^2 are discarded. The parameter h^2 measures the eccentricity of the coordinate system and should also be considered as a measure of the deformation of the nucleus, a result which shall be shown later for special models.

The dependence of the scattering amplitude on h^2 is contained in the geometrical factors $A_{ll'}{}^{m}$, which give the expansion of the spheroidal harmonics in terms of the spherical harmonics, and in the partial wave amplitudes η_{lm}. It will be recalled that the expansion of $A_{ll'}{}^{m}(h^2)$ is given by Eq. (21a)

$$A_{ll'}{}^{m}(h^2) = \delta_{ll'} + h^2\alpha_{ll'}{}^{m} + O(h^4). \quad (21a)$$

Similarly, the η_{lm} may be expanded in powers of the deformation parameter

$$\eta_{lm}(h^2) = \eta_l + h^2\eta_{lm}'(0) + O(h^4). \quad (35)$$

Here prime denotes differentiation with respect to h^2, and where it is explicitly recognized that $\eta_{lm}(0)$ is independent of m and equals η_l, the partial wave amplitude for the spherical nucleus.

The product of factors in Eq. (34) which are functions of h^2 may then be written, to first order in h^2,

$$(1-\eta_{lm}) A_{ll'}{}^{m} A_{ll''}{}^{m} \cong (1-\eta_l)\delta_{ll'}\delta_{ll''} + h^2[(1-\eta_l)(\alpha_{ll'}{}^{m}\delta_{ll''} + \alpha_{ll''}{}^{m}\delta_{ll'}) - \eta_{lm}'(0)\delta_{ll'}\delta_{ll''}]. \quad (36)$$

It is now apparent why it was advantageous to express the expansion coefficients $\alpha_{ll'}{}^{m}$ in terms of Clebsch-Gordan coefficients; the following orthogonality properties of these coefficients,

$$\sum_m (l\, I\, m\, 0\,|\, l\, m) = \delta_{I,0}(2l+1), \quad (37a)$$

$$\sum_m (l\, 2\, m\, 0\,|\, l'\, m)(l\, I\, m\, 0\,|\, l'\, m) = \delta_{I,2}(2l'+1)/5, \quad (37b)$$

enable one to evaluate the sum over m in Eq. (34) involving the first three terms of (36). In particular, it is found that

$$\sum_m \alpha_{ll'}{}^{m}(l\, 2\, m\, 0\,|\, l'\, m) = \frac{2}{15} \frac{[(2l+1)(2l'+1)]^{\frac{1}{2}}(l\, 2\, 0\, 0\,|\, l'\, 0)}{l(l+1)-l'(l'+1)}. \quad (38)$$

Thus, the scattering amplitude for the excitation of the $I=2^+$ level of the ground state rotational band becomes

$$f_{2M;00}(\theta,\phi) \cong i\lambda h^2(5\pi)^{\frac{1}{2}} \left\{ \frac{2}{15} \sum_{ll'} (\eta_{l'}-\eta_l) \frac{(2l+1)^{\frac{1}{2}}(l\, 2\, 0\, 0\,|\, l'\, 0)(l\, 2\, -M\, M\,|\, l'\, 0)}{l(l+1)-l'(l'+1)} Y_{l,-M}(\theta,\phi) - \sum_{lm} \eta_{lm}'(2l+1)^{-\frac{1}{2}}(l\, 2\, m\, 0\,|\, l\, m)(l\, 2\, -M\, M\,|\, l\, 0) Y_{l,-M}(\theta,\phi) \right\}. \quad (39)$$

To the same order, the elastic scattering amplitude is

$$f_{00;00}(\theta,\phi) \cong i\lambda\pi^{\frac{1}{2}} \sum_l \{(1-\eta_l)(2l+1)^{\frac{1}{2}} Y_{l,0}(\theta,\phi) - h^2\eta_{lm}'(2l+1)^{-\frac{1}{2}} Y_{l,0}(\theta,\phi)\}. \quad (40)$$

To this order in h^2 only the scattering amplitudes to the $I=0^+$ and 2^+ final states are non-vanishing since, as will be determined in the paragraphs which follow, the terms involving η_{lm}' also contribute only to the scattering amplitudes to these final states.

The preceding evaluation of these parts of the scattering amplitudes containing the geometrical factors has been straightforward. The evaluation of the remaining portions is less so, however, since it depends on the assumed form of η_{lm}.

As a guide to determine the form of η_{lm} the "radial equation" in spheroidal coordinates is recast so as to resemble the radial equations in spherical coordinates. Outside of the region of nuclear interaction the "radial equation" in spheroidal coordinates is given by Eq. (19a). The first derivatives in this differential equation may be eliminated by the substitution

$$J_{lm}(\xi)=(\xi^2-1)^{-\frac{1}{2}}u_{lm}(\xi), \tag{41}$$

so that the radial equation becomes

$$\frac{1}{h^2}\frac{d^2u_{lm}(\xi)}{d\xi^2}+\frac{\xi^2}{\xi^2-1}\left\{1-\frac{\Lambda_{lm}}{h^2\xi^2}-\frac{m^2-1}{h^2\xi^2(\xi^2-1)}\right\}u_{lm}(\xi)=0. \tag{42}$$

Similarly, the free-space radial equation in spherical coordinates is

$$\frac{1}{k^2}\frac{d^2u_l}{dr^2}+\left\{1-\frac{l(l+1)}{k^2r^2}\right\}u_l(r)=0. \tag{43}$$

The analogy between these two equations is apparent when it is recalled that in the limit $h\to 0$ (or $r\to\infty$), $h\xi\to kr$. To first order in h^2, the effective "centrifugal barrier" in Eq. (42) is

$$\frac{1}{(h\xi)^2}\left\{l(l+1)+h^2\left[\lambda_{lm}-1+\frac{m^2-1+l(l+1)}{h^2\xi^2}\right]\right\}. \tag{44}$$

The effective "angular momentum" $\mathfrak{L}_{lm}(h^2)$, at the point ξ, is defined accordingly by

$$\mathfrak{L}_{lm}(h^2)[\mathfrak{L}_{lm}(h^2)+1]\equiv l(l+1)+h^2\left[\lambda_{lm}-1+\frac{m^2-1+l(l+1)}{h^2\xi^2}\right]. \tag{45}$$

The fundamental assumption is now made, in analogy with the procedure followed in the monopole excitation section, that $\eta_{lm}(h^2)$ is a smooth monotonic function of $\mathfrak{L}_{lm}(h^2)$, i.e., $\eta_{lm}(h^2)=\eta(\mathfrak{L}_{lm}(h^2))$. A critical "angular momentum," L, is defined by the statement $\eta(L)=\frac{1}{2}$ and may be related to a critical surface ξ_c, through[18]

$$(h^2\xi_c^2)\equiv L(L+1). \tag{46}$$

It will have been noted that the effective "angular momentum," as here defined, is a function of ξ. It is now assumed that the $\mathfrak{L}_{lm}(h^2)$ occurring in η should be evaluated near the critical surface ξ_c. The motivation for this assumption is the belief[21,26] that the partial wave amplitudes are mainly determined by the amount of transmission into the nuclear interior allowed by the effective potential at and exterior to the nuclear surface.

When $\mathfrak{L}_{lm}(h^2)$ is evaluated at $\xi=\xi_c$, one obtains

$$\mathfrak{L}_{lm}(h^2)=l+\frac{h^2}{(2l+1)}\left\{(l\,2\,m\,0|l\,m)(l\,2\,0\,0|l\,0)\left[\frac{2}{3}-\frac{(2l-1)(2l+3)}{3L(L+1)}\right]+\frac{1}{3}\left[-2+\frac{4l(l+1)}{L(L+1)}\right]-\frac{1}{L(L+1)}\right\}. \tag{47}$$

On the other hand, when $\mathfrak{L}_{lm}(h)$ is evaluated at the classical turning point, i.e., the value of ξ such that the curly bracket of Eq. (42) vanishes, one finds

$$\mathfrak{L}_{lm}(h^2)=l+\frac{h^2}{(2l+1)}\left\{-(l\,2\,m\,0|l\,m)(l\,2\,0\,0|l\,0)\frac{2}{3}\left[\frac{l^2+l-\frac{3}{2}}{l(l+1)}\right]+\frac{2}{3}-\frac{1}{l(l+1)}\right\}. \tag{48}$$

The difference between these two forms is not of great practical consequence, since the main contributions to the scattering amplitude will come from partial waves with $l\approx L$ when there is a fairly rapid change from complete to no absorption around L.

The partial wave amplitude $\eta(\mathfrak{L}_{lm}(h^2))$ may be expanded

$$\eta_{lm}(h^2)\cong\eta_{lm}(0)+h^2\eta_{lm}'(0)=\eta(l)+[\mathfrak{L}_{lm}(h^2)-l](d/dl)\eta(l), \tag{49}$$

where $[\mathfrak{L}_{lm}(h^2)-l]$ is given either by Eqs. (47) or (48) above. The presence of the Clebsch-Gordan coefficients in these equations makes it possible through use of Eqs. (37a) and (37b) to carry out the sum over m in Eq. (39), so that

$$f_{2M;00}(\theta,\phi)\cong i\lambda h^2(5\pi)^{\frac{1}{2}}(2/15)\left\{\sum_{l,l'}[\eta(l')-\eta(l)]\frac{(2l+1)^{\frac{1}{2}}(l\,2\,0\,0|l'\,0)(l\,2\,-M\,M|l'\,0)}{l(l+1)-l'(l'+1)}Y_{l,-M}(\theta,\phi)\right.$$
$$\left.+\sum_l\frac{d\eta(l)}{dl}\left[\frac{l^2+l-\frac{3}{2}}{l(l+1)}\right](2l+1)^{-\frac{1}{2}}(l\,2\,0\,0|l\,0)(l\,2\,-M\,M|l\,0)Y_{l,-M}(\theta,\phi)\right\}, \tag{50}$$

[26] J. S. Blair, Phys. Rev. **108**, 827 (1957).

where Eq. (48) has been used for $\mathfrak{L}_{lm}(h^2)-l$. Similarly, the contributions to the elastic scattering amplitude, Eq. (40), of order h^2, may be evaluated; such terms will be dominated, however, by those which are independent of h^2. Thus in subsequent numerical work, the elastic scattering amplitude will be computed only to zeroth order in h^2; in other words, the usual spherical formula will be employed.

The inelastic scattering amplitude Eq. (50) can be evaluated for the sharp-cutoff approximation. Since the amplitudes η_l have meaning only for integral values of l, there is a certain amount of arbitrariness in one's definition of the sharp cutoff approximation. When $\eta(l)$ is taken to be a step function, then $d\eta(l)/dl$ is a δ function (at a point that might not even be defined). To circumvent this difficulty, the form of $d\eta(l)/dl$ will be chosen such that $\sum_l d\eta(l)/dl=1$, a result which becomes exact only when it is permissible to replace the sum by an integral over dl.

Thus for an integral value of L, the sharp-cutoff approximation is conveniently expressed as

$$\begin{aligned}\eta(l)&=0 \quad \text{for} \quad l<L,\\ &=\tfrac{1}{2}, \quad l=L,\\ &=1, \quad l>L,\end{aligned}$$

and

$$\begin{aligned}d\eta(l)/dl&=1 \quad \text{for} \quad l=L,\\ &=0 \text{ otherwise.}\end{aligned} \tag{51}$$

This is the form of the sharp-cutoff approximation which has been used in the discussion of monopole excitations (Sec. II). For half-integral values of L, it has been convenient to choose

$$\begin{aligned}\eta(l)&=0 \quad \text{for} \quad l<L,\\ &=1 \quad \text{for} \quad l>L,\end{aligned}$$

and

$$\begin{aligned}d\eta(l)/dl&=\tfrac{1}{2} \quad \text{for} \quad l=L\pm\tfrac{1}{2},\\ &=0 \text{ otherwise.}\end{aligned} \tag{52}$$

It is possible to establish the connection between the scattering amplitude given in the sharp-cutoff approximation and that calculated using the Frannhofer approximation. To show this connection it is worthwhile to evaluate explicitly Eq. (50) when the sharp-cutoff approximation is expressed by Eq. (52),

$$\begin{aligned}f_{2M;00}(\theta,\phi)\cong&-i\lambda h^2(5\pi)^{\frac{1}{2}}(1/15)\\ &\times\Big\{\frac{(2L'+1)^{\frac{1}{2}}}{2L'+3}(L'\,2\,0\,0|L'+2\,0)[(L'\,2\,-M\,M|L'+2\,0)Y_{L',-M}+(L'+2\,2\,-M\,M|L'\,0)Y_{L'+2,-M}]\\ &+\frac{(2L'-1)^{\frac{1}{2}}}{2L'+1}(L'-1\,2\,0\,0|L'+1\,0)[(L'-1\,2\,-M\,M|L'+1\,0)Y_{L'-1,-M}\\ &+(L'+1\,2\,-M\,M|L'-1\,0)Y_{L'+1,-M}]-\Big[\frac{L'^2+L'-\frac{3}{2}}{L'(L'+1)}\Big]\\ &\times(2L'+1)^{-\frac{1}{2}}(L'\,2\,0\,0|L'\,0)(L'\,2\,-M\,M|L'\,0)Y_{L',-M}\\ &-\Big[\frac{L'^2+3L'+\frac{1}{2}}{(L'+1)(L'+2)}\Big](2L'+3)^{-\frac{1}{2}}(L'+1\,2\,0\,0|L'+1\,0)(L'+1\,2\,-M\,M|L'+1\,0)Y_{L'+1,-M}\Big\},\end{aligned} \tag{53}$$

where to simplify the notation $L'\equiv L-\frac{1}{2}$.

It is interesting to examine this result when $L\gg 1$ and the scattering angle θ is small. Under these conditions, the spherical harmonics are well approximated by Bessel functions

$$Y_{L,M}(\theta,\phi)\to\Big[\frac{2L+1}{4\pi}\Big]^{\frac{1}{2}}J_{|M|}((L+\tfrac{1}{2})\theta)e^{iM\phi}\times\begin{Bmatrix}\text{times } (-)^M,\ M \text{ pos}\\ \text{times } (1),\ M \text{ neg}\end{Bmatrix} \tag{54}$$

and inspection of the formulas for the Clebsch-Gordan coefficients shows that they tend to simple numerical ratios. Dropping terms of order $1/L$, one finds

$$\begin{aligned}f_{2M;00}(\theta,\phi)\cong&-i\lambda\frac{5^{\frac{1}{2}}}{2}\frac{h^2}{15}J_0((L+\tfrac{1}{2})\theta) \quad \text{for} \quad M=0\\ \cong&0 \quad \text{for} \quad M=\pm 1\\ \cong&-i\lambda\frac{5^{\frac{1}{2}}}{2}\frac{h^2}{15}(\tfrac{3}{2})^{\frac{1}{2}}J_2((L+\tfrac{1}{2})\theta)\\ &\text{for} \quad M=\pm 2.\end{aligned} \tag{55}$$

In order to compare Eq. (55) to the scattering amplitude previously derived with use of the Fraunhofer ap-

proximation, it is desirable to relate the parameters h^2 and L to alternative characterizations of the nuclear deformation and radius. The spheroid $\xi=\xi_c$ can be approximated in polar coordinates by

$$R(\theta',\phi)=R_0[1+\beta_2 Y_{20}(\theta',\phi')] \\ =R_0[1+\epsilon P_2(\cos\theta')], \quad (56)$$

with

$$\xi_c\cong 2R_0/a \quad \text{and} \quad h^2\cong 3\epsilon(kR_0)^2=3(5/4\pi)^{\frac{1}{2}}\beta_2(kR_0)^2. \quad (57)$$

These relations may be combined with Eq. (46) to give

$$L+\tfrac{1}{2}=(h\xi_c)\cong kR_0. \quad (58)$$

Thus Eq. (55) becomes

$$f_{2M;00}(\theta,0)\cong -i(kR_0^2)\frac{\beta_2}{2(4\pi)^{\frac{1}{2}}}J_0(kR_0\theta) \quad \text{for} \quad M=0$$

$$\cong 0 \quad \text{for} \quad M=\pm 1$$

$$\cong -i(kR_0^2)\frac{\beta_2}{2(4\pi)^{\frac{1}{2}}}(\tfrac{3}{2})^{\frac{1}{2}}J_2(kR_0\theta) \quad \text{for} \quad M=\pm 2, \quad (59)$$

which is the inelastic scattering amplitude in the Fraunhofer approximation.[3,4,27]

When the linear approximation is used for the scattering amplitude, the cross sections for rotational excitation of an odd-A nucleus are related to those of an even-A nucleus in exactly the same manner as was indicated in earlier papers[4,28] on inelastic diffraction scattering. The differential scattering cross section between two states with total angular momenta I and I', which are members of the same rotational band corresponding to quantum number K, is given by

$$\frac{d\sigma}{d\Omega}(I\to I')=\delta_{I,I'}\frac{d\sigma_{\rm el}}{d\Omega}+(I\ 2\ K\ 0|I'\ K)^2\frac{d\sigma}{d\Omega}(0\to 2). \quad (60)$$

Here $d\sigma_{\rm el}/d\Omega$ and $(d\sigma/d\Omega)(0\to 2)$ are the expressions for the elastic and inelastic scattering cross sections from an even-A nucleus.

V. NUMERICAL APPLICATIONS

In the numerical examples of this section, the following simple form is adopted for η_l:

$$\eta(l)=\{1+\exp[-(l-L)/\Delta]\}^{-1}, \quad (61)$$

so that the angular distributions resulting from the evaluation of Eqs. (50) and (40) will be characterized by two adjustable parameters, the critical angular momentum L, and the width of the transition region, Δ. This choice has the following desirable features: (1) It is a simple expression which displays a gradual transition between strong to no absorption. (2) Analyses of elastic scattering cross sections by McIntyre *et al.*, using this form for partial wave amplitudes, have had some measure of success.[14]

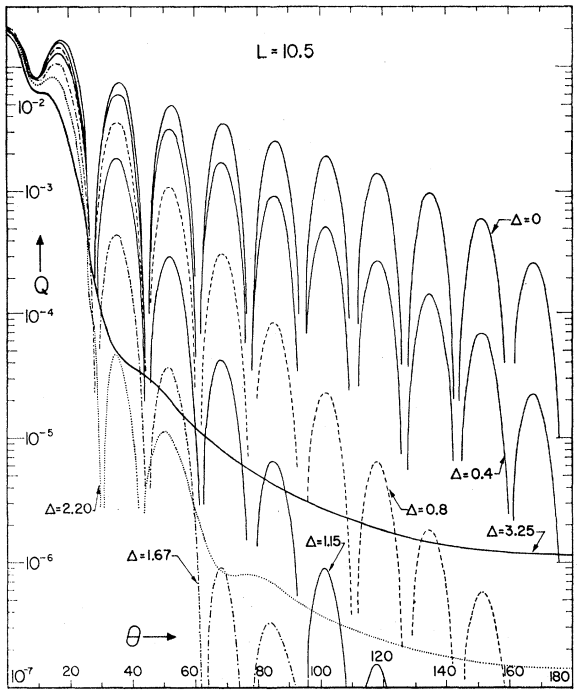

FIG. 1. Inelastic scattering cross sections for quadrupole excitation versus angle in degrees for $L=10.5$ and various values of Δ. The dimensionless ordinate, Q, is the differential cross section divided by $\beta_2^2(kR_0^2)^2$. Since L is a half integer, the cross section for $\Delta=0$ is computed using the prescription given by Eq. (52).

No attempt will be made in this paper to carry out exhaustive comparisons between this theory and experiment. Rather the numerical examples will illustrate the general features of the model.

To increase the import of the computed results, it is worthwhile to recall some of the predictions of the diffraction model in the Fraunhofer approximation[4]: (1) The computed differential cross sections displayed regularly spaced oscillations. (2) Except at the lowest orders of the diffraction pattern, there was a definite phase relationship between the elastic and inelastic angular distributions depending on the parity change of the excitation. (3) The angular distributions could be expressed in terms of "universal" curves, in the sense that the scattering cross sections, elastic and inelastic, when divided by $(kR_0^2)^2$, depended on k, R_0, and θ only through the argument, $kR_0\theta$ [or $2kR_0\sin(\theta/2)$], of the Bessel functions.

In Fig. 1 are plotted the inelastic scattering cross sections for quadrupole excitation versus angle for $L=10.5$ and various values of Δ. The dimensionless quantity shown is the square of the bracket of Eq. (50), summed over final states M; thus it is the differential

[27] S. I. Drozdov, J. Exptl. Theoret. Phys. (U.S.S.R.) **36**, 1875 (1959) [translation; Soviet Phys. JETP **9**, 1335 (1959)].
[28] S. I. Drozdov, J. Exptl. Theoret. Phys. (U.S.S.R.) **30**, 786 (1956) [translation; Soviet Phys. JETP **3**, 759 (1956)].

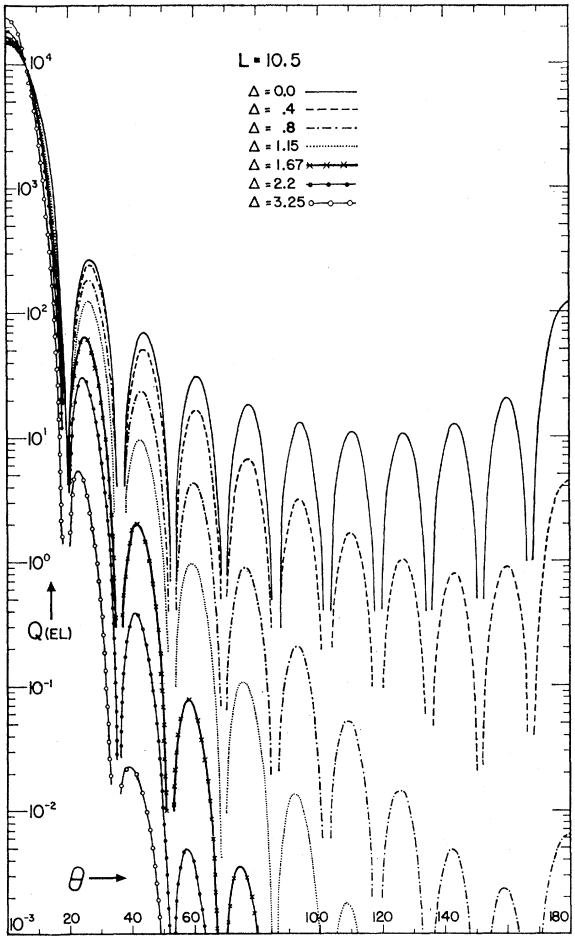

FIG. 2. The elastic scattering cross sections versus angle in degrees for $L=10.5$ and various values of Δ. The dimensionless ordinate $Q(\mathrm{EL})$ is the differential cross section times $(4k^2)$.

cross section divided by $[\chi\hbar^2(5\pi)^{\frac{1}{2}}(2/15)]^2=\beta_2^2(kR_0^2)^2$ and is denoted by Q. The following features will be observed: (a) The oscillations in the angular distributions have the same periodicity independent of Δ. (b) The cross sections are essentially equal at $\theta=0$ for all values of Δ. (c) As Δ is increased, the envelope of the oscillatory pattern drops off more rapidly with increasing angle. (d) For the largest values of Δ, the oscillatory structure at the higher orders of the diffraction pattern is completely damped out and the cross section flattens.

One frequent criticism of the Fraunhofer and sharp-cutoff models has been that they do not predict angular distributions which fall off at larger angles as rapidly as those frequently observed in nature. Feature (c) above supports one's feeling that this defect in the Fraunhofer and sharp-cutoff treatments is due to the assumed sharp nature of the transition.

For comparison, elastic scattering cross sections are given in Fig. 2 for $L=10.5$ as a function of Δ. The quantity plotted is the spherical cross section[14] multiplied by $(4k^2)$ and is denoted by $Q(\mathrm{EL})$,

$$Q(\mathrm{EL})=|\sum_l(2l+1)(1-\eta_l)P_l(\cos\theta)|^2. \qquad (62)$$

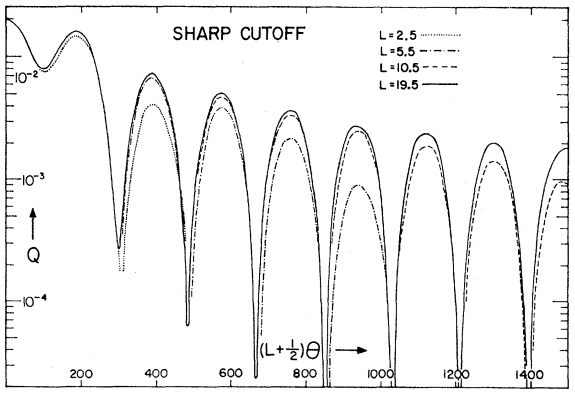

FIG. 3. The dimensionless inelastic cross section Q versus $(L+\frac{1}{2})\theta$ (where θ is in units of degrees) for $\Delta=0$ and various values of L.

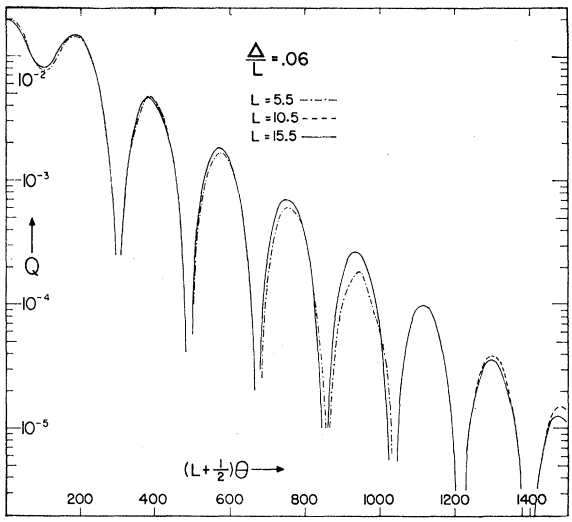

FIG. 4. The dimensionless inelastic cross section Q versus $(L+\frac{1}{2})\theta$ (where θ is in units of degrees) for $\Delta/L=0.06$ and various values of L.

The qualitative features of the inelastic scattering results are mirrored in the elastic scattering curves. It will be noted that the cross sections do not agree at $\theta=0$ but rather increase with Δ. This behavior is a consequence of the factor $(2l+1)$ in the elastic scattering amplitude; as Δ is increased this factor weights the partial waves with $l>L$.

Since the Fraunhofer results could be expressed in terms of "universal" curves, it appears worthwhile to consider whether similar constructions can be made for the present computations. A reasonable surmise is that cross sections calculated with different values of L but the same value of the ratio, Δ/L, should be closely related. Again the dimensionless inelastic scattering cross section Q (which is the true inelastic scattering cross

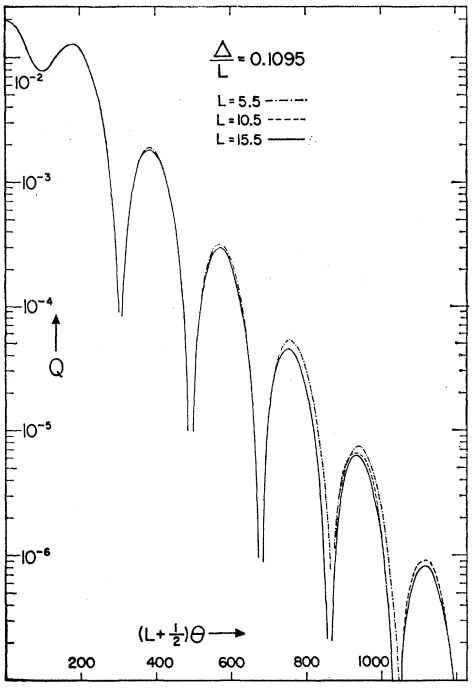

FIG. 5. The dimensionless inelastic cross section Q versus $(L+\frac{1}{2})\theta$ (where θ is in units of degrees) for $\Delta/L=0.1095$ and various values of L.

section divided by $\beta_2^2(kR_0^2)^2$ is plotted versus $(L+\frac{1}{2})\theta$ for various values of Δ/L in Figs. 3 through 7. Comparable results for elastic scattering are shown in Figs. 8 and 9 where $Q(\mathrm{EL})/(L+\frac{1}{2})^4=(d\sigma_{\mathrm{el}}/d\Omega)/[(kR_0^2)^2/4]$ is plotted versus $(L+\frac{1}{2})\theta$.

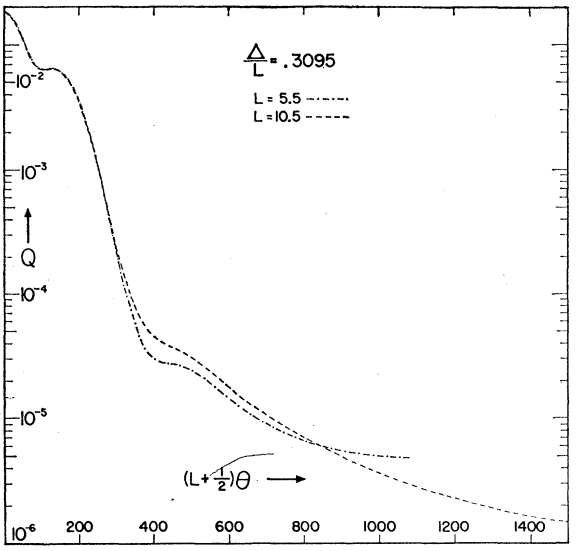

FIG. 7. The dimensionless inelastic cross section Q versus $(L+\frac{1}{2})\theta$ (where θ is in units of degrees) for $\Delta/L=0.3095$ and two values of L.

It will be seen that to a high degree of accuracy, it is possible to construct "universal" curves for the inelastic scattering cross sections and, to a lesser extent, such a construction is also possible for the elastic scattering cross sections. This means the two-parameter theory depends essentially on only one parameter Δ/L. To

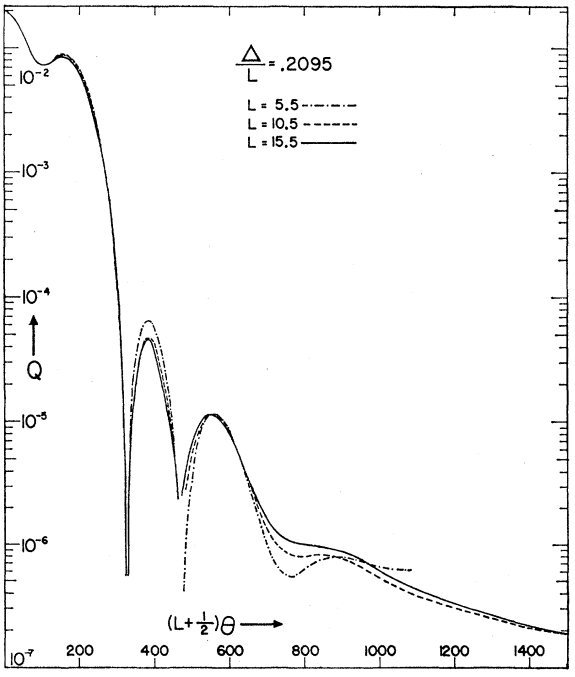

FIG. 6. The dimensionless inelastic cross section Q versus $(L+\frac{1}{2})\theta$ (where θ is in units of degrees) for $\Delta/L=0.2095$ and various values of L.

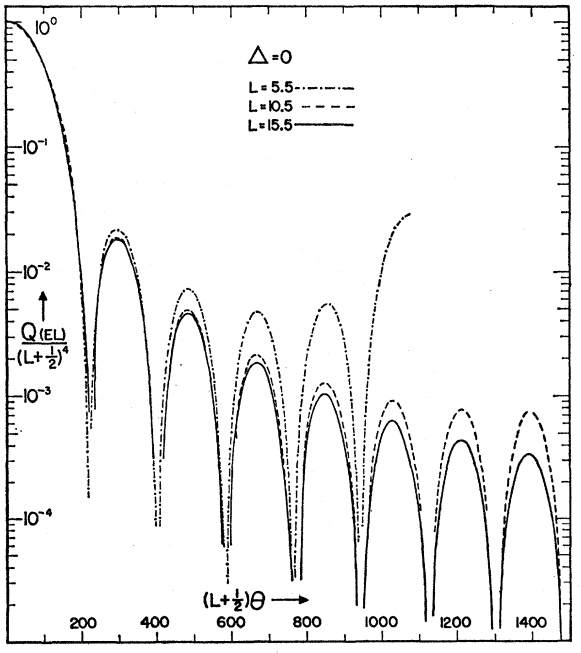

FIG. 8. The dimensionless elastic cross section $Q(\mathrm{EL})/(L+\frac{1}{2})^4$ versus $(L+\frac{1}{2})\theta$ (where θ is in units of degrees) for $\Delta=0$ and various values of L.

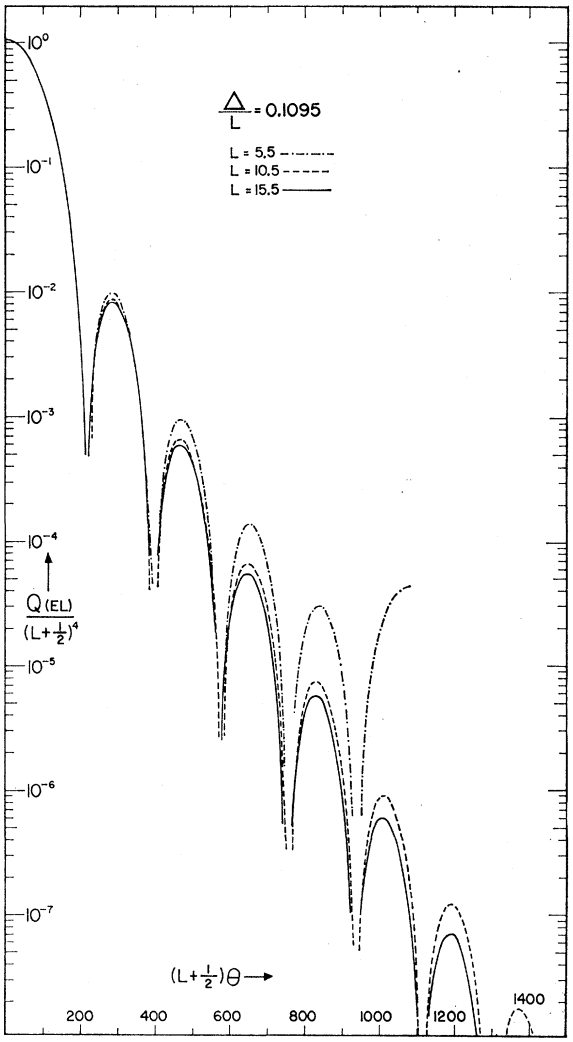

FIG. 9. The dimensionless elastic cross section $Q(\mathrm{EL})/(L+\frac{1}{2})^4$ versus $(L+\frac{1}{2})\theta$ (where θ is in units of degrees) for $\Delta/L=0.1095$ and various values of L.

facilitate use of this model in the analysis of experimental cross section, the computed inelastic and elastic scattering cross sections at the maxima are plotted versus Δ/L in Figs. 10 and 11, respectively. The separate curves are labeled by the parameter x which is the value of $(L+\frac{1}{2})\theta$ at the corresponding maxima of the Fraunhofer curves; to a very good approximation, the maxima for the cutoff models occur at the same values of $(L+\frac{1}{2})\theta$.

Some further remarks about these graphs follow: (a) The sharp-cutoff curves ($\Delta=0$) shown in Fig. 3 do not lie as close to one another as do those in the succeeding figures. The reason for this is that the sharp cutoff prescription given in Eq. (52), $d\eta_l/dl=\frac{1}{2}$ for $l=L\pm\frac{1}{2}$, partially simulates the effect due to a finite value of Δ. It is interesting to observe, nonetheless, that the cross section corresponding to a very small value of the critical angular momentum, $L=2.5$, bears considerable resemblance to the other curves.

(b) The Fraunhofer prediction for Q,[3,4]

$$Q=(1/4\pi)\{\tfrac{1}{4}J_0^2(kR_0\theta)+\tfrac{3}{4}J_2^2(kR_0\theta)\}, \qquad (63)$$

is practically indistinguishable from the sharp-cutoff curve for $L=19.5$ shown in Fig. 3. For example, the sixth maximum beyond $\theta=0$ in the Fraunhofer expression occurs at $(kR_0\theta)=1119.4$ degrees with $Q=2.60\times10^{-3}$; the corresponding maximum in the sharp-cutoff prediction for $L=19.5$ occurs at $(kR_0\theta)=1120$ degrees with $Q=2.38\times10^{-3}$. The agreement is much closer at small orders of the diffraction pattern. In an earlier paper[4] it was noted that the argument to be used in the Fraunhofer expressions was ambiguous and could depend on the choice of shadow plane. The comparison of the Fraunhofer and sharp-cutoff curves now shows that the appropriate argument at large angles is $kR_0\theta=(L+\frac{1}{2})\theta$. This conclusion also has been reached by Rost[29] through comparison of distorted-wave Born approximation computations and the Fraunhofer formula.

(c) The locations of the maxima and minima of the elastic scattering cross sections also are given very accurately by the corresponding Fraunhofer formula when $kR_0\theta=(L+\frac{1}{2})\theta$ is used as an argument. Since the elastic scattering cross sections do not possess "universality" to the extent which was evident for the inelastic scat-

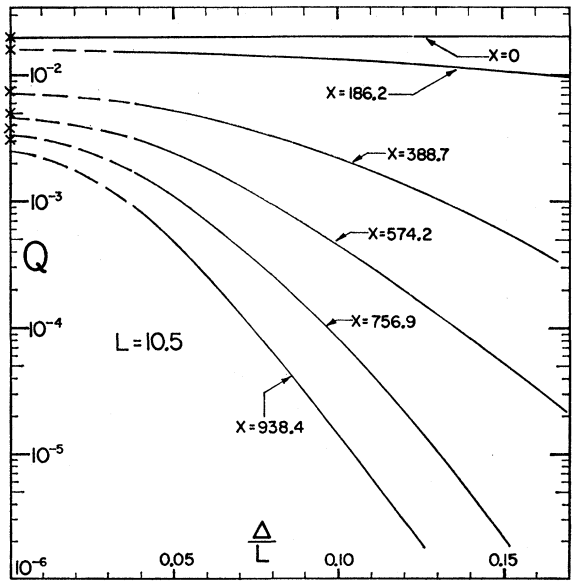

FIG. 10. The dimensionless inelastic cross section Q, at its maxima versus the ratio (Δ/L) for $L=10.5$. The separate curves are labeled by the parameter x which is the value of $(L+\frac{1}{2})\theta$ at the corresponding maxima of the Fraunhofer curves. The crosses on the $\Delta/L=0$ axis are the values of the Fraunhofer prediction for Q at these maxima. The dashed lines interpolate between $\Delta=0$ and $\Delta/L=0.04$ through a region where the computed cross sections were not considered meaningful; in this region the values of Δ are so small that the criterion $\sum_l d\eta(l)/dl\cong1$ is not well satisfied.

[29] E. Rost, Ph.D. thesis, University of Pittsburgh, 1961 (unpublished).

tering results, it is not surprising to find some deviation between the magnitudes of $Q(\mathrm{EL})/(L+\frac{1}{2})^4$ shown in Fig. 8 and the Fraunhofer prediction,

$$Q(\mathrm{EL})/(L+\tfrac{1}{2})^4=4[J_1(k_0R_0\theta)/(kR_0\theta)]^2. \quad (64)$$

For example, at the third maximum beyond $\theta=0$, the Fraunhofer prediction for this ratio is 1.6×10^{-3} while the sharp-cutoff result when $L=15.5$ is 1.8×10^{-3}. The agreement, of course, improves as L is increased.

(d) Both the elastic and inelastic scattering cross sections depart from their values at $\Delta=0$ in a similar fashion when considered as functions of (Δ/L). Let Figs. 8 and 9 be superimposed so that the ordinate at $\Delta=0$ for a maximum of given order on the elastic scattering figure lies midway between the corresponding ordinate for the maxima in the inelastic cross sections which bracket this order. It is then found that the elastic scattering curve smoothly interpolates between these two inelastic curves.

A standard technique used in calculating inelastic scattering cross sections has been the distorted-wave Born approximation (DWBA). Recent calculations by Rost and Austern[10,29,30] using this method have displayed many features of the Fraunhofer version of the inelastic diffraction model, such as the locations of the maxima and minima, and have provided good fits to several measured angular distributions of inelastically scattered alpha particles. To the extent that a potential description is relevant, the portion of the exact adiabatic inelastic scattering amplitude linear in the deformation parameter should be equivalent to the DWBA amplitude, computed for no energy transfer. The existing DWBA calculations contain some features which are not present in the linear deformation model of this paper, namely (a) consideration of deviations from the adiabatic condition (a consideration which lies outside the scope of an adiabatic calculation) and (b) inclusion of effects due to the Coulomb field (which, in principle, can be put into an adiabatic calculation).

It is worthwhile to attempt a comparison between the predictions with the DWBA model and the model of the present paper. In his thesis Rost has made a particularly detailed examination of the elastic and inelastic scattering of 43-Mev alpha particles from Ni^{60} using standard values for the optical potential. The relative location of the maxima and minima are in excellent agreement with the predictions of the Fraunhofer model (and consequently, also the smoothed-cutoff model). The magnitudes of the maxima in the computed DWBA angular distribution for quadrupole excitation may be compared to the smoothed-cutoff predictions plotted in Fig. 10. It is found that there is excellent agreement between the DWBA relative magnitudes and smoothed-cutoff predictions for the value $(\Delta/L)=0.48$. The only

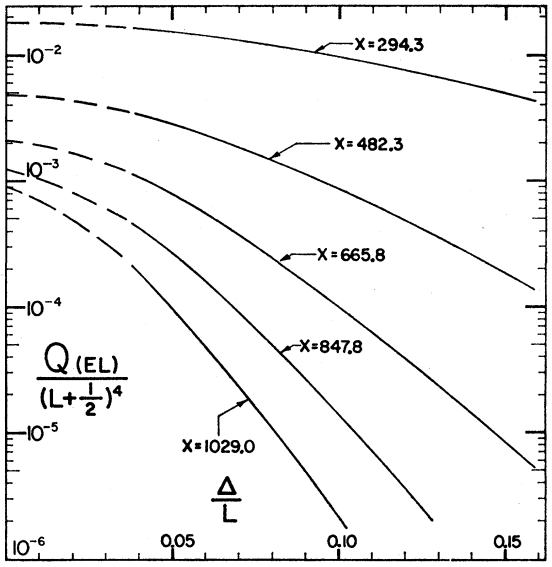

FIG. 11. The dimensionless elastic cross section $Q(\mathrm{EL})/(L+\frac{1}{2})^4$, at its maxima versus the ratio (Δ/L) for $L=10.5$. The separate curves are labeled by the parameter x which is the value of $(L+\frac{1}{2})\theta$ at the corresponding maxima of the Fraunhofer curves. The dashed lines interpolate between $\Delta=0$ and $\Delta/L=0.04$ through a region where the computed cross sections were not considered meaningful.

discrepancy among the first seven maxima occurred at 0° where the DWBA magnitude is about 10% less than the next maxima while the smoothed-cutoff magnitude at 0° is about 25% larger than the next maxima for $(\Delta/L)=0.48$. It is likely that this discrepancy is associated with the finite energy transfer and Coulomb excitation; these modifications were found[10,29] to be most effective near zero degrees.

For the example above, Rost has also given the magnitudes $|1-\eta_l|$ corresponding to the optical potentials employed. The values vary monotonically and, in the transition region, are fitted fairly well by the form of η_l given by Eq. (61), where L is slightly larger than 19 and $\Delta\cong1.0$ with about a 10% uncertainty. It will be noted that the resulting ratio, $\Delta/L\cong0.05$, is in accord with that determined in the paragraph above.

This comparison leads us to make the following observations: As can be seen from inspection of Eqs. (8) and (50), our inelastic as well as the elastic cross sections depend only on the functional form of the partial wave amplitudes. The optical model provides a mechanism for generating partial wave amplitudes. Indeed, for a suitable choice of parameters the optical model yields partial wave amplitudes resembling the simple form used in the present computations and a full DWBA computation using those optical model wave functions is in good accord with the computations of this section. Any other physical model, however, for which the partial wave amplitudes vary in a similarly smooth fashion[31]

[30] N. Austern, *Proceedings of the Seventh International Conference on Nuclear Structure, Kingston, 1960* (University of Toronto Press, Toronto, Canada, 1960), p. 323.

[31] An illuminating argument justifying a smoothed transition in the partial wave amplitude, with no appeal made to the optical model, has been provided recently by Austern in reference 21.

will yield roughly the same inelastic scattering cross sections. Thus it is by no means clear at this stage that calculations with a complex local potential provide a uniquely successful description of a strongly absorbing nucleus.

Although no detailed fits to experimental results will be given, two comparisons to Fig. 10 will be cited:

(1) "Universal" plots have been made[6] of several angular distributions for alpha particles which excite the 1.37-Mev 2^+ state of Mg^{24}. The relative magnitudes of the maxima corresponding to $x=388.7$, 574.2, and 756.9 degrees indicate that $(\Delta/L)\cong 0.05$; comparison of the maxima at $x=186.2$ and 388.7 degrees alone yields a larger value, $\Delta/L\cong 0.08$. When the smoothed cutoff calculations are used, the values of the collective parameters are altered slightly from values obtained using the Fraunhofer formulas. When (Δ/L) is set equal to 0.05 and a fit between theory and experiment is made at $x=388.7$ degrees, the value of $(\beta_2 R_0)$ is altered from[32] 1.43f to 1.70f, in close agreement with the DWBA value 1.67f.

(2) The maxima in the angular distributions[5] of 41-Mev alpha particles which excite the lowest 2^+ states of natural Ni may be compared to Fig. 10. The falloff from the Fraunhofer prediction for the maxima is matched rather well by the value $(\Delta/L)\cong 0.06$.

To conclude this section, the reader should be reminded of the many approximations and omissions in these calculations: (a) The adiabatic approximation itself takes no account of the oftentimes large energy transfer. (b) There has been no consideration of Coulomb distortion of the incident wave nor Coulomb excitation. (c) A very simple form was chosen to represent the partial wave amplitudes. Even the expansion of $\eta_{lm}(h^2)$ given by Eq. (49) required that there be a simple functional dependence. (d) Lastly, only terms in the scattering amplitude linear in the deformation have been retained. This approximation is particularly suspect at large angles; indeed, the experimenter is cautioned against taking too seriously any attempt to obtain detailed fits between observed angular distributions spanning a wide range of angles and theories whose scattering amplitudes are no more than linear in the deformation. Some of these questions are reconsidered in the next section.

[32] J. S. Blair, *Proceedings of the Seventh International Conference on Nuclear Structure, Kingston, 1960* (University of Toronto Press, Toronto, Canada, 1960), p. 824.

VI. POSSIBLE EXTENSIONS

The underlying basis of the present model is the adiabatic approximation. Once this has been assumed, one is quite at liberty in choosing the partial wave amplitudes η_{lm} according to any physical model.

In the context of the present work, there are several obvious extensions:

(1) Although the linear (small-deformation) approximation was considered here for simplicity of computation, the apparatus needed for calculation in a spheroidal coordinate system with arbitrary deformation is available in this paper and the literature.

(2) An attempt was made to include Coulomb effects. The wave equation does separate in spheroidal coordinates with a potential generated by a pair of point charges located at the foci of the coordinate ellipsoids. It was found, however, that the electric quadrupole moment of such a charge distribution is roughly five times that due to a uniformly charged ellipsoid with the same distortion of the nuclear surface and thus gives rise to spurious Coulomb excitation comparable with the nuclear potential excitation being calculated. For this reason the work was not pursued further, although there may well be methods to circumvent the difficulty.

(3) In general, the partial wave amplitudes (for example, as derived from optical potentials) are complex, and the variation in phase as well as magnitude should be included.

(4) The correspondence between the sharp-cutoff and Fraunhofer models has now been established for both elastic and (rotational) inelastic scattering. It should also be possible to establish similar correspondences between the smooth-cutoff model and a diffuse-surface Fraunhofer model.

ACKNOWLEDGMENTS

The authors are grateful to Mr. Warren Brown for the programming and execution of most of the numerical computations. They also wish to express thanks to John Wills and Thomas Miller for assistance in preparation of the figures and to Dr. E. S. Rost for providing a copy of his thesis.